Fermi Resonances of Borohydrides in a Crystalline Environment of Alkali Metals

Philippe Carbonnière*,† and Hans Hagemann‡

Laboratoire de Chimie Théorique et Physico-Chimie Moléculaire, UMR 5624, Fédération de Recherche IPREM 2606, Université de Pau et des Pays de l'Adour, IFR Rue Jules Ferry, 64000, Pau, France, and Département de Chimie Physique, Université de Genève, 30, quai E. Ansermet, CH 1211 Geneva 4 Switzerland

Vibrational spectra of BH_4^- and its isotopic analogues in a crystalline environment of alkali metals cations (K^+, Rb^+, Cs^+) have been investigated beyond the harmonic approximation using a variational approach supported by computations of B3LYP type anharmonic force fields. From the comparison of the observed and simulated IR spectra, the influence of the anharmonic couplings on the band position and on the relative intensity of the allowed vibrational transitions is discussed. Here, the effect of the crystalline environment induces a blue shift of about 50 and 100 cm^{-1} respectively for the bending and stretching modes of BH_4^-. Furthermore, anharmonic effects, which are exclusively well reproduced by a variational approach, are needed to yield reliable positions and relative amplitudes of IR allowed combination and overtone transitions. This leads to theoretical results fitting their experimental counterpart between 6 and 30 cm^{-1} in the investigated series.

Introduction

Ternary hydrides are the subject of intensive investigations in the field of on-board storage of hydrogen for fuel cell applications for automotive use.[1] Of special interest are hydrides which release hydrogen at practical temperatures and pressures. For instance, Ti-doped $NaAlH_4$ can undergo a two-step reversible decomposition through Na_3AlH_6 to $NaH + Al$, with a theoretical capacity of 5.6 wt %.[2]

Borohydrides can potentially provide even higher capacities, but the simple ternary borohydrides such as $NaBH_4$ appear to be rather stable with decomposition temperatures above 300 °C. Very recently, a compound stemming from the reaction of $LiBH_4$ and $LiNH_2$ was shown to present hydrogen desorption exceed 10 wt %.[3]

These promising results stimulate more fundamental research on the properties of borohydrides and aluminum hydrides. The crystal structures of alkali metal borohydrides have been studied using X-ray and neutron diffraction;[4] more recently the structural transitions of $NaBH_4$ under pressure have been investigated.[5] In conjunction with these crystallographic studies, vibrational spectra have also been obtained. Systematic frequency shifts with the nature of the alkali (and/or the size of the unit cell) are observed.[4,6] The inelastic neutron scattering spectra of $NaBH_4$ and KBH_4 have been studied in conjunction with periodic DFT calculations[7] which provide good predictions of the low-frequency internal vibrations of the BH_4^- ion in these crystals.

In this work, we investigate the vibrational spectra of $^{11}BH_4^-$ and its isotopic analogues ($^{11}BD_4$, $^{10}BH_4^-$, and $^{10}BD_4^-$) in a crystalline environment using anharmonic DFT calculations. These theoretical results are compared with experimental IR spectra.[4] Strong anharmonic couplings were observed for this molecule. Thus, a study beyond the harmonic approximation appears to be necessary to render, at least qualitatively, a correct description of the band shifts induced by Fermi resonances and of their relative intensity. Unlike the second-order perturbation theory approach (hereafter PT2), which fails in the case of too strong anharmonic couplings, the variational treatment is exact while considering all the excitations of the vibrational levels of interest, for a given Hamiltonian. On the basis of our experience (see ref 8 and therein), configurations interaction (hereafter CI) of single, double, triple, and quadruple excitations yields a good estimation of the nature and the weight of vibrational configurations mixed in each vibrational state. This is the treatment considered here.

Computational Details

Anharmonic quartic force field of $^{11}BH_4^-$ and its isotopes ($^{10}BH_4^-$, $^{11}BD_4^-$, $^{10}BD_4^-$) was determined with Gaussian 03 package[9] by finite difference of $6N$-11 analytic Hessians (N being the number of atoms) around the optimized geometry. Here we recall[10] that the best compromise between different error sources is obtained using a step size of 0.010 Å in the numerical differentiation of harmonic frequencies, tight geometry optimizations and fine grids (at least 99 radial and 590 angular points) for the numerical integration of the functional.

According to vibrational studies investigating semirigid organic molecular systems[11,12] the B3LYP/6-31+G(d,p) model was chosen to compute anharmonic force constants in reason for its ability to fit accurate quantum mechanical methods such as CCSD(T)[13]/cc-pVTZ[14] model.

Although the use of CCSD(T) level of theory is generally recommended to drive harmonic computations, the harmonic study of the naked anion reported in Table 1 reveals that B3LYP/6-31+G(d,p)[15] is able to match its CCSD(T)/aug-ccpVTZ counterpart by less than 15 cm^{-1}. As a matter of fact, harmonic computations of MBH_4 species (M = K, Rb, Cs) and their isotopes was also performed by B3LYP level of theory using

* Corresponding author.Telephone: 33(0)5-59-40-78-58. Fax: 33(0)5-59-40-78-62. E-mail: philippe.carbonniere@univ-pau.fr.
† Laboratoire de Chimie Théorique et Physico-Chimie Moléculaire, UMR 5624, Fédération de Recherche IPREM 2606, Université de Pau et des Pays de l'Adour.
‡ Département de Chimie Physique, Université de Genève.

TABLE 1: Comparison between CCSD(T)/aug-ccpVTZ Harmonic Frequencies of BH_4^- Species and Their B3LYP/6-31+G(d,p) Counterpart

		CCSD(T)/aug-ccpVTZ				B3LYP/6-31+G(d,p)			
mode	sym	$^{11}BH_4^-$	$^{10}BH_4^-$	$^{11}BD_4^-$	$^{10}BD_4^-$	$^{11}BH_4^-$	$^{10}BH_4^-$	$^{11}BD_4^-$	$^{10}BD_4^-$
ω_1	A_1	2266	2266	1603	1603	2280	2280	1612	1612
ω_2	E	1203	1203	851	851	1194	1194	845	845
ω_3	F_2	2253	2263	1670	1686	2247	2257	1666	1681
ω_4	F_2	1085	1095	825	834	1080	1089	821	830

TABLE 2: Harmonic (ω) and Anharmonic (ν) Frequencies of BH_4^- Species Computed at the B3LYP/6-31+G(d,p) Level of Theory (in cm^{-1}): Comparison with Experimental Values

		$^{11}BH_4^-$			$^{10}BH_4^-$			$^{11}BD_4^-$			$^{10}BD_4^-$		
mode	sym	ω	ν	exp[a]	ω	ν	exp[b]	ω	ν	exp[b]	ω	ν	exp[b]
1	A_1	2280	2203	*2312[b]*	2280	2208		1612	1537	*1592[b]*	1612	1540	*1597[b]*
				2287[c]						*1578[c]*			
2	E	1194	1159	*1246[b]*	1194	1159		845	827	*892[b]*	845	827	
				1220[c]						*871[c]*			
3	F_2	2247	2137	*2288[b]*	2257	2147		1666	1575	*1672[b]*	1681	1589	*1688[b]*
				2255[c]						*1648[c]*			
4	F_2	1080	1046	*1119[b]*	1089	1055	*1126[b]*	821	803	*852[b]*	830	812	*861[b]*
				1103[c]			*1111[c]*			*839[c]*			*850[c]*

[a] exp = taken from ref 4. [b] Raman frequencies of KBH_4 at room temperature. [c] Raman frequencies of $CsBH_4$ at room temperature.

TABLE 3: Optimized Geometry (in Å) Calculated at the B3LYP/(6-31+G(d,p)/LANL2DZ) Level of Theory for MBD_4 Compounds[a]

	KBD_4		$RbBD_4$		$CsBD_4$	
	our work	exp	our work	exp	our work	exp
D_{MD}	2.864	$2.795_{(LT)*8}$	3.065	$2.922_{(LT)*24}{}^a$	3.295	$3.106_{(LT)*24}{}^a$
		$2.770_{(LT)*4}$				
		$2.837_{(HT)*24}{}^a$		$2.980_{(HT)*24}{}^a$		$3.161_{(HT)*24}{}^a$
D_{BD}	1.225	$1.205_{(LT)*4}$	1.226	$1.221_{(LT)*4}$	1.228	$1.215_{(LT)*4}$
		$1.196_{(HT)*4}$		$1.206_{(HT)*4}$		$1.217_{(HT)*4}$

[a] D site occupancy $^1/_2$. All crystallized structures are cfc ($Fm3m$) expect for KBD_4 at 10 K (tetragonal, $P42/nmc$). [b] Comparison with experimental data at 1.5 K (LT) and 295 K (HT).[4]

the 6-31+G(d,p) for the anion and LANL2DZ[16] for the surrounding.

The vibrational Schrödinger equation was solved by variational procedure considering the rotational contribution to anharmonicity[17] in the Watson Hamiltonian.[18] The corresponding IC matrix going up to hexaexcitations of fundamental configuration, was then diagonalized in a basis set of harmonic oscillators product.

Harmonic IR intensities have also been computed at this level of theory despite the weakness of the basis set used. Furthermore, anharmonic intensities have been estimated by considering the sum of harmonic intensities related to the configurations describing each vibrational state under investigation weighted by their contributions. IR spectrum of each compound is then built by considering a 5 cm^{-1} wide Lorentzian distribution of rovibrational states, centered on the calculated transitions.

Results and Discussion

The presence of strong coupling between adjacent internal mode energy levels is an important feature of the spectra of borohydrides. An anharmonic study is then essential to correctly represent the position of transitions and above all, the relative intensity of overtones and combination bands arising by resonances. Thus, fair determination of anharmonic force constants, accurate description of zero-order vibrational problem

and reliable vibrational treatment are a pre requisite, since as illustrated by the well-known second-order perturbation formula (PT2):

$$E_{\Psi i} = \langle \Psi_i^0 | \hat{H} | \Psi_i^0 \rangle + \sigma \frac{\langle \Psi_i^0 | \hat{H} | \Psi_j^0 \rangle^2}{E_i^0 - E_j^0}$$

E_{Ψ_i}: energy of the vibrational state i

Ψ_a^0, configuration a: zero-order eigenfunction, solution of harmonic vibrational treatment

E_a^0: zero-order energy

Fermi resonance occurs between two configurations i and j for $E_i^0 \approx E_j^0$, which leads to a failure of vibrational treatment by current PT2 approach.

A. Vibrational Transition of the Naked Anion. As a first step of the investigation, B3LYP/6-31+G(d,p) harmonic and anharmonic results of the naked BH_4^- anion, and its isotopes are reported in Table 2 and compared to experimental values[4] obtained by Raman spectra of KBH_4 and $CsBH_4$ at room temperature (cfc structure). The picture clearly shows that anharmonic results are far by about 100 cm^{-1} below the experimental values for most of frequencies so that harmonic frequencies are artificially closer to experimental observations. As mentioned above, the accuracy of the DFT model seems not involved since a such model leads to results typically fitting

Fermi Resonances of Borohydrides

J. Phys. Chem. A, Vol. 110, No. 32, 2006 **9929**

TABLE 4: Significant Third and Fourth Derivatives (cm^{-1}), in Dimensionless Normal Coordinates Space, Responsible for Resonances and Corresponding Anharmonic Transitions (cm^{-1})

derivatives	$^{11}BH_4^-$	$^{10}BH_4^-$	$^{11}BD_4^-$	$^{10}BD_4^-$
ϕ_{111}	−653	−653	−388	−388
ϕ_{333}	846	856	549	556
ϕ_{122}	60	56	33	33
ϕ_{144}	165	167	106	107
ϕ_{344}	−97	−105	−51	−55
ϕ_{234}	87	75	47	47
ϕ_{1133}	213	215	112	114
ϕ_{2433}	0	0	−45	−45
ν_1 (A_1)	2203 68% ν_1 + 17% $2\nu_4$	2208 64% ν_1 + 21% $2\nu_4$	1537 67% ν_1 + 24% $2\nu_4$	1540 72% ν_1 + 18% $2\nu_4$
ν_3 (F_2)	2137 46% ν_3 + 33% $2\nu_4$ + 13% $\nu_4 + \nu_2$	2147 47% ν_3 + 34% $2\nu_4$ + 8% $\nu_4 + \nu_2$	1575 58% ν_3 + 17% $2\nu_4$ + 8% $\nu_4 + \nu_2$	1589 62% ν_3 + 24% $2\nu_4$ + 10% $\nu_4 + \nu_2$
$2\nu_4$ (A_1)	2062 79% $2\nu_4$ + 16% ν_1 + 1% $2\nu_1$	2076 75% $2\nu_4$ + 20% ν_1 + 2% $2\nu_1$	1626 73% $2\nu_4$ + 20% ν_1 + 2% $2\nu_1$	1640 77% $2\nu_4$ + 14% ν_1 + 4% $2\nu_2$
$2\nu_4$ (E)	2092 97% ν_4	2110 97% ν_4	1606 97% ν_4	1624 97% ν_4
$2\nu_4$ (F_2)	2072 62% $2\nu_4$ + 1% $\nu_2 + \nu_4$ + 32% ν_3	2085 60% $2\nu_4$ + 1% $\nu_2 + \nu_4$ + 32% ν_3	1614 52% $2\nu_4$ + 18% $\nu_2 + \nu_4$ + 11% ν_3	1630 66% $2\nu_4$ + 25% $\nu_2 + \nu_4$ + 5% ν_3
$2\nu_2$ (A_1)	2319 97% $2\nu_2$	2318 97% $2\nu_2$	1654 97% $2\nu_2$	1653 93% $2\nu_2$ + 2% ν_1
$\nu_2 + \nu_4$ (F_2)	2219 82% $\nu_2 + \nu_4$ + 12% ν_3 + 2% $\nu_1 + \nu_3$	2228 82% $\nu_2 + \nu_4$ + 20% ν_3 + 5% $2\nu_4$	1641 73% $\nu_2 + \nu_4$ + 20% ν_3 + 5% $2\nu_4$	1654 52% $\nu_2 + \nu_4$ + 26% ν_3 + 17% $2\nu_4$
$2\nu_1$ (A_1)	4419 23% $2\nu_1$ + 24% $\nu_1 + 2\nu_4$ + 3% ν_1...	4435 18% $2\nu_1$ + 23% $\nu_1 + 2\nu_4$ + 5% ν_1...	3064 36% $2\nu_1$ + 39% $\nu_1 + 2\nu_4$ + 5% ν_1...	3074 45% $2\nu_1$ + 32% $\nu_1 + 2\nu_4$ + 5% ν_1...
$\nu_1 + \nu_3$ (F_2)	4290 30% $\nu_1 + \nu_3$ + 2% ν_3...	4294 20% $\nu_1 + \nu_3$ + 3% ν_3...	3102 35% $\nu_1 + \nu_3$ + 21% $3\nu_4$ + 3% ν_3...	3122 40% $\nu_1 + \nu_3$ + 20% $3\nu_4$ + 4% ν_3...
$2\nu_3$ (A_1)	4215 41% $2\nu_3$ + 34% $4\nu_4$ + 2% ν_1...	4242 36% $2\nu_3$ + 28% $4\nu_4$ + 2% ν_1...	3133 34% $2\nu_3$ + 3% $2\nu_1$ + 2% ν_1...	3156 27% $2\nu_3$ + 10% $2\nu_1$ + 3% ν_1...

experimental data by 5−15 cm^{-1} as observed on small molecular systems (H_2CO, H_2CS, CH_2NH, C_2H_4, CH_3Li, ...)[11,19,20] as well as on larger organic systems (benzene, pyrrole, furan, thiophene, azabenzenes, and uracyle).[11,21−23] The discrepancies observed shows that surrounding in a solid strongly hinders the motions of vibrations of the central species which explains the too low calculated energies by considering the naked form of BH_4^- with regard to experimental values. This is in agreement with experimental investigation of alkali borohydride series, where frequencies of the anion clearly decrease while the octahedral site is widened from KBH_4 to $CsBH_4$.[4]
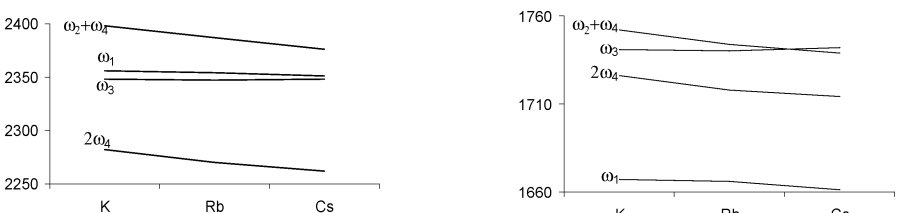
The strong Fermi resonances are essentially observed in the bond stretching region at 2100−2400 and 1600−1800 cm^{-1}, respectively, for $[BH_4]^-$ and $[BD_4]^-$ complexes. It concerns the ν_1 (A_1) symmetric stretching mode and the ν_3 (F_2) asymmetric stretching mode mixed with adjacent overtones and combination bands of the ν_4 (F_2) and ν_2 (E) transitions (respectively asymmetric and symmetric bending mode).

As mentioned by Memon et al.[24] in a study of boro-hydrides and deuterides isolated in alkali halides, IR transitions involving F_2 sublevels of $2\nu_4$ and $\nu_2 + \nu_4$ appear strongly because of the resonance with ν_3. Likewise, strong coupling occurs between $2\nu_4$ (A_1) and ν_1 transition in Raman spectrum. Anharmonic calculations on the naked species reveal the same trend. As reported in Table 4, the $2\nu_4$ state includes about 15−20% of ν_1 configuration through the ϕ_{122} third derivative estimated at 165 and 105 cm^{-1} for hydrides and deuterides, respectively. Conversely, this coupling yields enough $2\nu_4$ character to the predominantly ν_1 transition to separate out the ^{10}B and ^{11}B components by about 5 cm^{-1} for hydrides and 3 cm^{-1} for deuterides, close to experimental observations (respectively 8 cm^{-1} [4] and 5 cm^{-1} [18]).

F_2 sublevels of $2\nu_4$, $\nu_2 + \nu_4$, and ν_3 are connected via Fermi resonances, through ϕ_{344} and ϕ_{234} derivatives (estimated around 90 and 50 cm^{-1} for ^1H and ^2D species, respectively). Note that Darling−Dennisson resonances may also occur because of the promiscuity of $2\nu_4$ and $\nu_2 + \nu_4$ transitions through the ϕ_{24ii} type quartic derivatives ($i \in [1,4]$). Surprisingly, a significant $\phi_{2433} = -45$ cm^{-1} is observed in the anharmonic force field of deuterides even though it appears equal to zero for hydrides. This yields a 3 configurations/3 interactions system for deuterides vs a 3 configurations/2 interactions system for hydrides which contributes to explain the marked differences of the ν_3 character observed in $2\nu_4$ and $\nu_2 + \nu_4$ for these two isotopic species.

B. Vibrational Transition of MBH$_4$ Species. Anharmonic force field of the naked species seems, at least qualitatively, able to reproduce the resonances reported experimentally. Nevertheless, it clearly appears that the influence of the surroundings have to be considered for further accurate computations, keeping in mind that reasonable computational cost is required. In this connection, a simple model of the cfc MBH_4 species (M = K, Rb, Cs) was invoked, including the central BH_4^- anion and its first neighbors made by an octahedral environment of alkali metals.

These undeca-atomic systems were optimized in T_d symmetry applying a global neutral charge, followed by a harmonic frequency calculation. Optimized B−D and M−D bond lengths of deuterides are reported in the Table 3 and compared with their experimental counterpart stemmed from neutron diffraction study.[4] The theoretical M−D distances, in any case appreciably greater than the observed values: 0.069, 0.143, and 0.189 Å, respectively, for K, Rb, and Cs species. This reveals an anion less crowded in the model compared to the real system.

TABLE 5: Harmonic Frequencies for KBH$_4$, RbBH$_4$, CsBH$_4$, and their Isotopic species (in cm^{-1})^a

ω_i	sym	KBH$_4$	RbBH$_4$	CsBH$_4$	*BH$_4^-$*	KBD$_4$	RbBD$_4$	CsBD$_4$	*BD$_4^-$*
ω_4	F$_2$	1141	1135	1131	*1080*	863	859	857	*821*
$^{10}\omega_4$	F$_2$	1150	1144	1141	*1089*	872	868	867	*830*
ω_2	E	1257	1252	1245	*1194*	889	885	882	*845*
$^{10}\omega_2$	E	1257	1252	1245	*1194*	889	885	882	*845*
ω_3	F$_2$	2348	2347	2348	*2247*	1741	1740	1742	*1666*
$^{10}\omega_3$	F$_2$	2359	2358	2362	*2257*	1757	1756	1760	*1681*
ω_1	A$_1$	2356	2354	2351	*2280*	1667	1666	1661	*1612*
$^{10}\omega_1$	A$_1$	2356	2354	2351	*2280*	1667	1666	1661	*1612*

^{a} Comparison to naked compounds.

Furthermore, the gap increases from KBH$_4$ to CsBH$_4$ while the cation becomes less electronegative. Note also that, unlike experimental observations, B−D distances are poorly affected by the nature of the alkali metal. These show the limit of the model.

Harmonic frequency calculations of all the structures are reported in Table 5 and compared to the results obtained for the corresponding anions. Here, matrix effects in salts of BH$_4^-$ can be estimated to 50−100 cm^{-1} respectively for bending and stretching mode: an order of magnitude comparable to anharmonicity effects, much more important than in solution where a shift of 5−30 cm^{-1} is typically observed. Note that the stretching modes value is quite constant in the alkali series investigated while bending modes frequency decrease by about 10 cm^{-1} from K to Cs. Thereby, the $\omega_4 + \omega_2$ draw nearer to ω_1 and ω_3 from K to Cs while the $2\omega_4$ withdraws for hydride compounds. This is in agreement with the corresponding experimental IR spectra (see Figure 1.) where the relative intensity of the $2\nu_4$ (F$_2$) with regard to ν_3 decreases while the $\nu_4 + \nu_2$ grow from a more marked ν_3 character along the series. The same picture is observed in Raman spectra by comparing the $2\nu_4$ (A$_1$) with respect to the ν_1. Harmonic frequencies of deuterides species yield the same progression of the ω's, expected that ω_1 is too low in energy comparatively to $2\omega_2$. This suggests a very weak interaction between this two modes and then probably no evidence of the $2\nu_2$ (A$_1$) transition in the corresponding Raman spectra.[4]

Although qualitative interpretation of alkali hydrides and deuterides spectra is proposed on this basis of a harmonic study, a poorly rendered position, both absolute and relative, of the
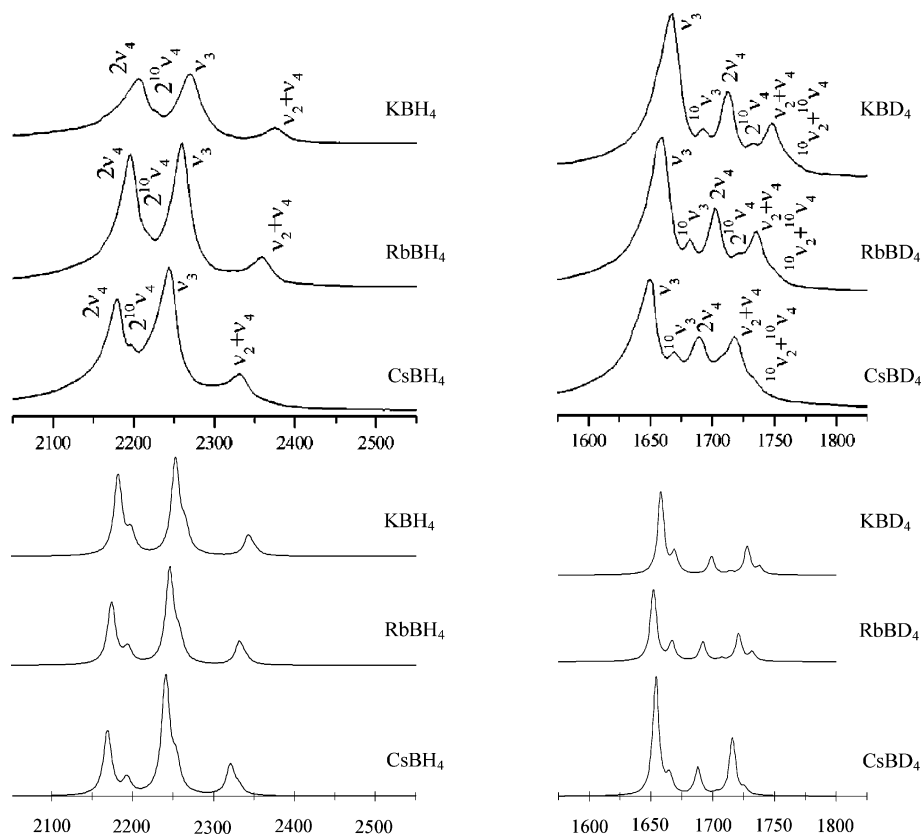

Figure 1. Experimental and theoretical IR spectra of MBH$_4$ (M = K, Rb, Cs).

TABLE 6: Calculated Fundamental Transitions for KBH$_4$, RbBH$_4$, CsBH$_4$, and Their Isotopic Species (in cm^{-1})

ν_i	sym	KBH$_4$ our work		exp	KBD$_4$ our work		exp	RbBH$_4$ our work		exp	RbBD$_4$ our work		exp	CsBH$_4$ our work		exp	CsBD$_4$ our work		exp
ν_4	F$_2$	1106	97% ν_4 / 2% $\nu_1+\nu_4$	1112[a] 1119[b]	845	97% ν_4 / 2% $\nu_1+\nu_4$	848[a] 852[b]	1100	97% ν_4 / 2% $\nu_1+\nu_4$	1106[a] 1112[b]	841	98% ν_4 / 2% $\nu_1+\nu_4$	843[a] 847[b]	1097	97% ν_4 / 2% $\nu_1+\nu_4$	1094[a] 1103[b]	839	98% ν_4 / 2% $\nu_1+\nu_4$	836[a] 839[b]
$^{10}\nu_4$	F$_2$	1114	97% ν_4 / 2% $\nu_1+\nu_4$	1126[b]	854	97% ν_4 / 2% $\nu_1+\nu_4$	860[a] 861[b]	1109	97% ν_4 / 2% $\nu_1+\nu_4$	1125[a] 1120[b]	850	98% ν_4 / 2% $\nu_1+\nu_4$	859[a]	1107	97% ν_4 / 2% $\nu_1+\nu_4$	1111[a] 1111[b]	848	98% ν_4 / 2% $\nu_1+\nu_4$	849[a] 850[b]
ν_2	E	1221	96% ν_2 / 3% $\nu_1+\nu_2$	1246[b]	872	97% ν_2 / 2% $\nu_1+\nu_2$	892[b]	1216	96% ν_2 / 3% $\nu_1+\nu_2$	1234[b]	868	97% ν_2 / 2% $\nu_1+\nu_2$	883[b]	1210	96% ν_2 / 3% $\nu_1+\nu_2$	1220[b]	863	97% ν_2 / 2% $\nu_1+\nu_2$	871[b]
$^{10}\nu_2$	E	1221	96% ν_2 / 3% $\nu_1+\nu_2$	1246[b]	872	97% ν_2 / 2% $\nu_1+\nu_2$	892[b]	1216	96% ν_2 / 3% $\nu_1+\nu_2$	1234[b]	868	97% ν_2 / 2% $\nu_1+\nu_2$	883[b]	1210	96% ν_2 / 3% $\nu_1+\nu_2$	1220[b]	863	97% ν_2 / 2% $\nu_1+\nu_2$	871[b]
ν_3	F$_2$	2253	44% ν_3 / 41% $2\nu_4$ / 10% $\nu_2+\nu_4$	2270[a] 2288[b]	1658	62% ν_3 / 25% $2\nu_4$ / 6% $\nu_2+\nu_4$	1668[a] 1672[b]	2246	47% ν_3 / 34% $2\nu_4$ / 12% $\nu_2+\nu_4$	2260[a] 2273[b]	1652	57% ν_3 / 30% $2\nu_4$ / 7% $\nu_2+\nu_4$	1659[a] 1662[b]	2241	51% ν_3 / 23% $2\nu_4$ / 12% $\nu_2+\nu_4$	2244[a] 2255[b]	1654	52% ν_3 / 35% $2\nu_4$ / 7% $\nu_2+\nu_4$	1650[a] 1648[b]
$^{10}\nu_3$	F$_2$	2265	43% ν_3 / 40% $2\nu_4$ / 8% $\nu_2+\nu_4$		1669	64% ν_3 / 23% $2\nu_4$ / 8% $\nu_2+\nu_4$	1693[a] 1688[b]	2258	47% ν_3 / 34% $2\nu_4$ / 12% $\nu_2+\nu_4$		1667	60% ν_3 / 26% $2\nu_4$ / 9% $\nu_2+\nu_4$	1682[a] 1678[b]	2254	48% ν_3 / 30% $2\nu_4$ / 14% $\nu_2+\nu_4$		1665	57% ν_3 / 31% $2\nu_4$ / 10% $\nu_2+\nu_4$	1669[a]
ν_1	A$_1$	2296	60% ν_1 / 27% $2\nu_4$ / 6% $2\nu_1$	2312[b]	1600	75% ν_1 / 16% $2\nu_4$ / 5% $2\nu_1$	1592[b]	2292	63% ν_1 / 24% $2\nu_4$ / 7% $2\nu_1$	2300[b]	1597	73% ν_1 / 18% $2\nu_4$ / 5% $2\nu_1$	1586[b]	2284	63% ν_1 / 24% $2\nu_4$ / 7% $2\nu_1$	2287[a]	1592	74% ν_1 / 17% $2\nu_4$ / 5% $2\nu_1$	1578[b]
$^{10}\nu_1$	A$_1$	2303	54% ν_1 / 33% $2\nu_4$ / 6% $2\nu_1$		1603	78% ν_1 / 14% $2\nu_4$ / 6% $2\nu_1$	1597[b]	2298	58% ν_1 / 30% $2\nu_4$ / 6% $2\nu_1$		1600	77% ν_1 / 13% $2\nu_4$ / 6% $2\nu_1$		2292	58% ν_1 / 30% $2\nu_4$ / 6% $2\nu_1$		1595	77% ν_1 / 13% $2\nu_4$ / 6% $2\nu_1$	

[a] Comparison to observed IR transitions. Only the most relevant configurations describing each state have been reported for sake of clarity. [b] Comparison to observed Raman transitions. Only the most relevant configurations describing each state have been reported for sake of clarity.

TABLE 7: Calculated Combination Bands and Overtones for KBH$_4$, RbBH$_4$, CsBH$_4$ and Their Isotopic Species (in cm^{-1}):

ν_i	sym	KBH$_4$ our work		exp	KBD$_4$ our work		exp	RbBH$_4$ our work		exp	RbBD$_4$ our work		exp	CsBH$_4$ our work		exp	CsBD$_4$ our work		exp
$2\nu_4$	A$_1$	2174	69% $2\nu_4$	2181^b	1706	82% $2\nu_4$	1710^b	2165	72% $2\nu_4$	2166^b	1699	80% $2\nu_4$	1700^b	2157	73% $2\nu_4$	2149^b	1695	80% $2\nu_4$	1685^b
			25% ν_1			14% ν_1			22% ν_1			15% ν_1			22% ν_1			15% ν_1	
			2% $2\nu_1$			1% $2\nu_1$			2% $2\nu_1$			1% $2\nu_1$			2% $2\nu_1$			1% $2\nu_1$	
$2^{10}\nu_4$	A$_1$	2185	63% ν_4	- / -	1721	84% ν_4	- / 1726^b	2177	67% ν_4	- / 2175^b	1715	84% ν_4	- / 1715^b	2171	67% $2\nu_4$	- / 2157^b	1710	83% ν_4	- / -
			30% ν_1			10% ν_1			27% ν_1			11% ν_1			28% ν_1			11% ν_1	
			3% $2\nu_1$						3% $2\nu_1$						3% $2\nu_1$				
$2\nu_4$	E	2213	97% $2\nu_4$	- / -	1690	98% $2\nu_4$	- / -	2201	97% $2\nu_4$	- / -	1682	98% $2\nu_4$	- / -	2193	97% $2\nu_4$	- / -	1678	98% $2\nu_4$	- / -
			2% $\nu_1+2\nu_4$			2% $\nu_1+2\nu_4$			1% $\nu_1+2\nu_4$						2% $\nu_1+2\nu_4$				
$2^{10}\nu_4$	E	2230	97% $2\nu_4$	- / -	1708	98% $2\nu_4$	- / -	2219	97% $2\nu_4$		1701	98% $2\nu_4$	- / -	2213	97% $2\nu_4$	- / -	1697	98% $2\nu_4$	- / -
			1% $\nu_1+2\nu_4$						1% $\nu_1+2\nu_4$						1% $\nu_1+2\nu_4$				
$2\nu_4$	F$_2$	2182	55% $2\nu_4$	2208^a 2217^b	1699	65% $2\nu_4$	1713^a -	2174	61% $2\nu_4$	2196^a 2202^b	1692	59% $2\nu_4$	- 1703^a	2170	67% $2\nu_4$	2179^a 2183^b	1688	58% $2\nu_4$	1689^a -
			37% ν_3			13% ν_3			31% ν_3			15% ν_3			28% ν_3			12% ν_3	
			3% $\nu_1+\nu_3$			19% $\nu_2+\nu_4$			3% $\nu_1+\nu_3$			19% $\nu_2+\nu_4$			2% $\nu_1+\nu_3$			28% $\nu_2+\nu_4$	
$2^{10}\nu_4$	F$_2$	2198	51% $2\nu_4$	2231^a 2231^b	1714	60% $2\nu_4$	1733^a -	2194	60% $2\nu_4$	2225^a 2217^b	1707	53% $2\nu_4$	1721^a -	2193	65% $2\nu_4$	2197^a 2194^b	1703	53% $2\nu_4$	1704^a -
			40% ν_3			7% ν_3			32% ν_3			8% ν_3			27% ν_3			8% ν_3	
			3% $\nu_1+\nu_3$			31% $\nu_2+\nu_4$			2% $\nu_1+\nu_3$			40% $\nu_2+\nu_4$			2% $\nu_1+\nu_3$			41% $\nu_2+\nu_4$	
$\nu_2+\nu_4$	F$_2$	2343	86% $\nu_2+\nu_4$	2376^a 2384^b	1728	73% $\nu_2+\nu_4$	1748^a 1748^b	2332	84% $\nu_2+\nu_4$	2359^a 2365^b	1721	65% $\nu_2+\nu_4$	1736^a 1733^b	2321	82% $\nu_2+\nu_4$	2332^a 2341^b	1716	62% $\nu_2+\nu_4$	1719^a 1716^b
			9% ν_3			21% ν_3			11% ν_3			22% ν_3			13% ν_3			25% ν_3	
						4% $2\nu_4$						8% $2\nu_4$						6% $2\nu_4$	
$^{10}\nu_2+\nu_4$	F$_2$	2351	84% $\nu_2+\nu_4$	- / -	1739	66% $\nu_2+\nu_4$	1761^a -	2340	83% $\nu_2+\nu_4$	- / -	1732	55% $\nu_2+\nu_4$	1750^a	2331	81% $\nu_2+\nu_4$		1726	55% $\nu_2+\nu_4$	1750^a
			9% ν_3			22% ν_3			11% ν_3			27% ν_3			13% ν_3			18% ν_3	
			10% $2\nu_4$									15% $2\nu_4$						15% $2\nu_4$	
$2\nu_2$	A$_1$ E	2439 2447	96% $2\nu_2$	- 2505^b	1740 1744	96% $2\nu_2$	- 1774^b	2429 2437	96% $2\nu_2$	- 2481^b	1734 1738	98% $2\nu_2$	- 1753^b	2420 2423	96% $2\nu_2$	- 2450^b	1726 1728	97% $2\nu_2$	- 1732^b
			3% $\nu_1+2\nu_2$			2% $\nu_1+2\nu_2$			3% $\nu_1+2\nu_2$			2% $\nu_1+2\nu_2$			2% $\nu_1+2\nu_2$			2% $\nu_1+2\nu_2$	
$2^{10}\nu_2$	A$_1$ E	2439 2448	96% $2\nu_2$	2505^b	1740 1744	96% $2\nu_2$	1774^b	2430 2436	96% $2\nu_2$	2481^b	1733 1737	98% $2\nu_2$	1753^b	2420 2423	96% $2\nu_2$	2450^b	1727 1731	97% $2\nu_2$	- 1732^b
			3% $\nu_1+2\nu_2$			2% $\nu_1+2\nu_2$			3% $\nu_1+2\nu_2$			2% $\nu_1+2\nu_2$			2% $\nu_1+2\nu_2$			2% $\nu_1+2\nu_2$	
absolute mean shift				30			15			22			12			13			6
relative mean shift^c				98.4			98.9			98.9			99.1			99.4			99.6

^{a} Comparison to observed IR transitions. Only the most relevant configurations describing each state have been reported for sake of clarity ^{b} Comparison to observed Raman transitions. Only the most relevant configurations describing each state have been reported for sake of clarity ^{c} Absolute/relative mean shift in cm^{-1}/percent; based on Raman data.

Fermi Resonances of Borohydrides

J. Phys. Chem. A, Vol. 110, No. 32, 2006 **9933**

fundamental transitions force us to lead further investigations beyond the harmonic approximation. As example, ω_1 and ω_3 are too close in energy and their correct progression with respect to the nature of the alkali metal can be only explained by a fair estimation of Fermi resonances. In this connection, it has been shown in a recent study on solvent effect in vibrational transitions[25] that discrepancies between anharmonic force constants determined in gas phase and in implicit solvent lead to minor modifications of the final values. On the basis of this assumption, the quartic force fields of MBH_4 compounds were built by superposition of the harmonic part of the surrounded species and the anharmonic part of the naked anions. Results of vibrational treatment by the IC approach are reported in Tables 6 and 7 and show a clear improvement of the theoretical values. As expected, the model is as much reliable as the electrostatic force decreases between the anion and the alkali metal since an agreement of 98.4%, 98.9%, and 99.4% is observed for KBH_4, $RbBH_4$, $CsBH_4$, respectively, i.e., an absolute mean discrepancy of 30, 22, and 13 cm^{-1} for the series.

For a clearer understanding of resonances that appear, the simulated IR spectra of the species based on the eigenvectors analysis issuing from the IC procedure are reported in Figure 1 and compared to their experimental counterpart. We recall that in the spectral range considered, all the allowed transitions result from their ν_3 character exclusively; as consequence the relative intensities of the bands are directly deduced from the value of its contribution. Furthermore, the relative amount of the two isotopes in natural boron (19.6% of ^{10}B and 80.4% of ^{11}B) was applied. The progressions of the $2\nu_4$ and $\nu_2 + \nu_4$ intensity relative to ν_3 are fairly traduced. The first decreases while the second increases: 37%, 31%, 28% of ν_3 character in the $2\nu_4$ and 9%, 11%, and 13% in the $\nu_2 + \nu_4$ for the ^{11}hydrides series. Concerning the ^{11}deuterides, we report 13%, 15%, and 12% of ν_3 character for $2\nu_4$ and 21%, 22%, and 25% for $\nu_2 + \nu_4$. As already mentioned, these lower contributions relative to those observed for hydride species could be related to the presence of Darling-Dennisson coupling that occurs between $2\nu_4$ and $\nu_2 + \nu_4$. This is in agreement with the IR experimental spectra. Note also the ratio in frequency ν_1^H/ν_1^D (equal to $\sqrt{2}$ in absence of anharmonic resonances) is calculated at 1.44, whatever the alkali metal, fairly close to the experimental value (1.45).

Conclusion

Vibrational spectra of BH_4^- and its isotopic analogues have been investigated in a K^+, Rb^+, and Cs^+ crystalline environment by an variational anharmonic approach. The model which consists of a central BH_4^- anion surrounded by an octahedral environment of alkali metals is as much reliable as the ionic strength decreases between BH_4^- and its counterion. The average discrepancy between theoretical and experimental data go from 1.5% for KBH_4 species to reach 0.5% for $CsBH_4$, i.e., less than 13 cm^{-1} in absolute value.

Furthermore, we have shown the following:

The importance of anharmonic effects inclusion by variational approach to properly reproduce the shape of the IR spectra, principally structured by anharmonic couplings, as well as the balance of the bands in the series.

The crystalline environment effects are not negligible; their magnitudes reach in the present case the values of anharmonicities and blue shift the transitions. As a consequence,

observed transitions of alkali borohydrides are closer to the harmonic values of the corresponding naked anion, which is purely fortuitous.

It is nevertheless clear that a correct determination of line widths and overlaps requires a rovibrational analysis, namely to attempt to model the temperature dependence on this parameter as observed in Raman spectra of alkali borohydrides species. A reliable determination of Raman intensities at the harmonic level is then essential (all fundamental transitions and combination bands arising from them are allowed) and requires a more extended basis set for polarizability computations. Work is in progress in our laboratories along this and related directions.

References and Notes

(1) Schlapbach, L.; Züttel, A. *Nature (London)* **2001**, *414*, 353.

(2) Bogdanovic, B.; Schwickardi, M. *J. Alloys Compd.* **1997**, *253*, 1.

(3) Pinkerton, F. E.; Meisner, G. P.; Meyer, M. S.; Balogh, M. P.; Kundrat, M. D. *J. Phys. Chem. B.* **2005**, *109*, 6.

(4) Renaudin, G.; Gomes, S.; Hagemann, H.; Keller, L.; Yvon, K. *J. Alloys Compd.* **2004**, *375*, 98.

(5) Kumar, R. S.; Cornelius, A. L. *Appl. Phys. Lett.* **2005**, *87*, 261916.

(6) Hagemann, H.; Gomes, S.; Renaudin, G.; Yvon, K. *J. Alloys Compd.* **2004**, *363*, 126.

(7) Allis, D. G.; Hudson, B. S. *Chem. Phys. Lett.* **2004**, *385*, 166.

(8) Begue, D.; Carbonniere, P.; Pouchan, C. *J. Phys. Chem. A* **2005**, *109*, 4611.

(9) Frisch, M. J.; Trucks, G. W.; Schlegel, H. B.; Scuseria, G. E.; Robb, M. A.; Cheeseman, J. R.; Montgomery, J. A., Jr.; Vreven, T.; Kudin, K. N.; Burant, J. C.; Millam, J. M.; Iyengar, S. S.; Tomasi, J.; Barone, V.; Mennucci, B.; Cossi, M.; Scalmani, G.; Rega, N.; Petersson, G. A.; Nakatsuji, H.; Hada, M.; Ehara, M.; Toyota, K.; Fukuda, R.; Hasegawa, J.; Ishida, M.; Nakajima, T.; Honda, Y.; Kitao, O.; Nakai, H.; Klene, M.; Li, X.; Knox, J. E.; Hratchian, H. P.; Cross, J. B.; Bakken, V.; Adamo, C.; Jaramillo, J.; Gomperts, R.; Stratmann, R. E.; Yazyev, O.; Austin, A. J.; Cammi, R.; Pomelli, C.; Ochterski, J. W.; Ayala, P. Y.; Morokuma, K.; Voth, G. A.; Salvador, P.; Dannenberg, J. J.; Zakrzewski, V. G.; Dapprich, S.; Daniels, A. D.; Strain, M. C.; Farkas, O.; Malick, D. K.; Rabuck, A. D.; Raghavachari, K.; Foresman, J. B.; Ortiz, J. V.; Cui, Q.; Baboul, A. G.; Clifford, S.; Cioslowski, J.; Stefanov, B. B.; Liu, G.; Liashenko, A.; Piskorz, P.; Komaromi, I.; Martin, R. L.; Fox, D. J.; Keith, T.; Al-Laham, M. A.; Peng, C. Y.; Nanayakkara, A.; Challacombe, M.; Gill, P. M. W.; Johnson, B.; Chen, W.; Wong, M. W.; Gonzalez, C.; Pople, J. A.; Gaussian 03, Revision C.02, Gaussian, Inc., Wallingford CT, 2004.

(10) Barone, V. *J. Chem. Phys.* **2005**, *122*, 014108.

(11) Carbonniere, P.; Lucca, T.; Pouchan, C.; Rega-N.; Barone, V. *J. Comput. Chem.* **2005**, *26*, 384.

(12) Carbonniere, P.; Barone, V. *Chem. Phys. Lett.* **2004**, *399*, 226.

(13) Raghavachri, K.; Trucks, G. W.; Pople, J. A.; Head-Gordon, M. *Chem. Phys. Lett.* **1989**, *157*, 479.

(14) Kendall, R. A.; Dunning, T. H.; Jr; Harrison, R. J. *J. Chem. Phys.* **1992**, *96*, 6769.

(15) Clark, T.; Chandrasekhar, J.; Spitznagel, G. W.; Schleyer, P. v. R. *J. Comput. Chem.* **1983**, *4*, 294.

(16) Hay, P. J.; Wadt, W. R. *J. Chem. Phys.* **1985**, *82*, 299.

(17) Carbonniere, P.; Barone, V. *Chem. Phys. Lett.* **2004**, *392*, 365.

(18) Watson, J. K. G. *Mol. Phys.* **1968**, *15*, 479.

(19) Gohaud, N.; Begue, D.; Pouchan, C. *Chem. Phys.* **2005**, *310*, 85.

(20) Boese, A. D.; Klopper, W.; Martin, J. M. L. *Int. J. Quantum Chem.* **2005**, *104*, 830.

(21) Boese, A. D.; Martin, J. M. L. *J. Phys. Chem. A* **2004**, *108*, 3085.

(22) Barone, V. *Chem. Phys. Lett.* **2004**, *383*, 528.

(23) Barone, V.; Festa, G.; Grandi, A.; Rega, N.; Sanna, N. *Chem. Phys. Lett.* **2004**, *388,* 279.

(24) Memon, M. I.; Sherman, W. F.; Wilkinson, G. R. *Spectrosc. Acta* **1981**, *37*, 461.

(25) Begue, D.; Carbonniere, P.; Barone, V.; Pouchan, C. *Chem. Phys. Lett.* **2005**, *416*, 206.